Technical Review

No. 2 · 1987

Recent Developments in Accelerometer Design
Trends in Accelerometer Calibration

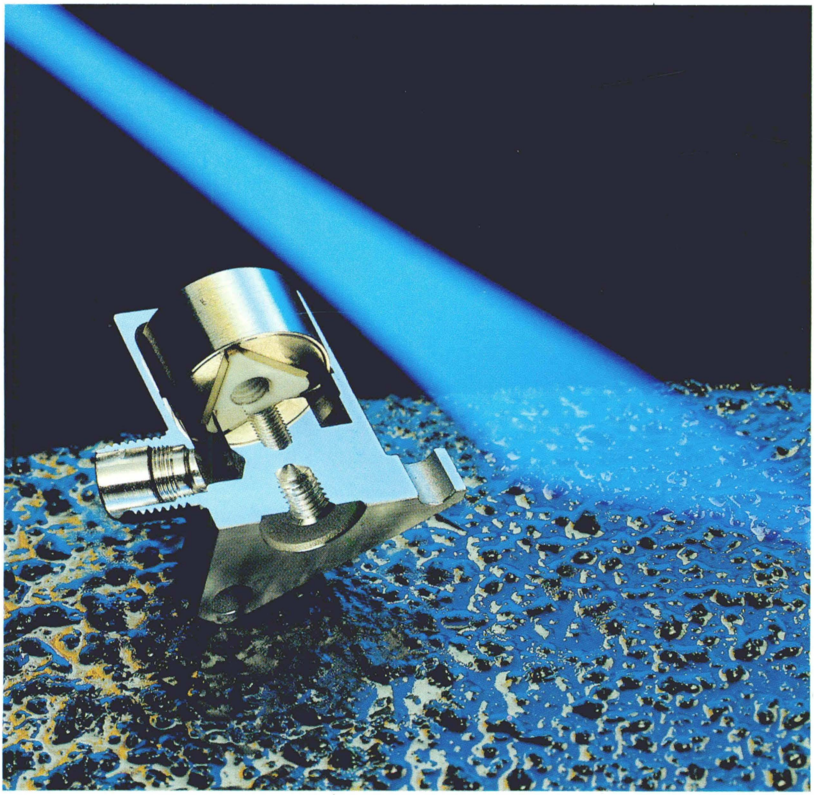

Brüel & Kjær

Previously issued numbers of Brüel & Kjær Technical Review

1-1986 Vibration Monitoring of Machines
4-1986 Field Measurements of Sound Insulation with a Battery-Operated Intensity Analyzer
Pressure Microphones for Intensity Measurements with Significantly Improved Phase Properties
Measurement of Acoustical Distance between Intensity Probe Microphones
Wind and Turbulence Noise of Turbulence Screen, Nose Cone and Sound Intensity Probe with Wind Screen
3-1986 A Method of Determining the Modal Frequencies of Structures with Coupled Modes
Improvement to Monoreference Modal Data by Adding an Oblique Degree of Freedom for the Reference
2-1986 Quality in Spectral Match of Photometric Transducers
Guide to Lighting of Urban Areas
1-1986 Environmental Noise Measurements
4-1985 Validity of Intensity Measurements in Partially Diffuse Sound Field
Influence of Tripods and Microphone Clips on the Frequency Response of Microphones
3-1985 The Modulation Transfer Function in Room Acoustics
RASTI: A Tool for Evaluating Auditoria
2-1985 Heat Stress
A New Thermal Anemometer Probe for Indoor Air Velocity Measurements
1-1985 Local Thermal Discomfort
4-1984 Methods for the Calculation of Contrast
Proper Use of Weighting Functions for Impact Testing
Computer Data Acquisition from Brüel & Kjær Digital Frequency Analyzers 2131/2134 Using their Memory as a Buffer
3-1984 The Hilbert Transform
Microphone System for Extremely Low Sound Levels
Averaging Times of Level Recorder 2317
2-1984 Dual Channel FFT Analysis (Part II)
1-1984 Dual Channel FFT Analysis (Part I)
4-1983 Sound Level Meters – The Atlantic Divide
Design principles for Integrating Sound Level Meters
3-1983 Fourier Analysis of Surface Roughness
2-1983 System Analysis and Time Delay Spectrometry (Part II)
1-1983 System Analysis and Time Delay Spectrometry (Part I)
4-1982 Sound Intensity (Part II Instrumentation and Applications)
Flutter Compensation of Tape Recorded Signals for Narrow Band Analysis
3-1982 Sound Intensity (Part I Theory).
2-1982 Thermal Comfort.
1-1982 Human Body Vibration Exposure and its Measurement.

(Continued on cover page 3)

Technical Review

No. 2 · 1987

Contents

Recent Developments in Accelerometer Design 1
by Torben R. Licht
Henrik Andersen
and Henrik Brill Jensen

Trends in Accelerometer Calibration 23
by Torben R. Licht
Henrik Andersen

Recent Developments in Accelerometer Design

by Torben R. Licht,
Henrik Andersen and
Henrik Brill Jensen

Abstract

Two-channel FFT analysis is used to evaluate the performance of various accelerometer designs. The measurements demonstrate the importance of using the frequency spectrum for evaluation of the environmental performance of transducers. Furthermore, the superior environmental-performance characteristics of the Brüel & Kjær Delta Shear® piezoelectric accelerometer design as compared to other designs are demonstrated.

Sommaire

L'analyse FFT bicanale est utilisée pour évaluer les performances de diverses conceptions d'accéléromètres. Les mesures montrent l'importance de l'utilisation des spectres de fréquences pour l'évaluation de la sensibilité des capteurs à l'environnement. De plus, on démontre dans ce domaine, la supériorité de la conception Cisaillement en Delta des capteurs piezoélectriques Brüel & Kjær comparée à d'autres conceptions.

Zusammenfassung

Mit der Zweikanal-FFT-Analyse kann das Verhalten von Beschleunigungsaufnehmern mit verschiedenen Konstruktionsprinzipien beurteilt werden. Die Meßergebnisse zeigen die Bedeutung des Frequenzspektrums zur Bewertung der Umwelteinflüsse. Das vorzügliche Verhalten auf Umwelteinflüsse von Brüel & Kjær-Beschleunigungsaufnehmern mit Delta-Scher®-Bauweise wird mit Aufnehmern anderer Bauweise verglichen.

Introduction

In recent years vibration problems associated with advances in structural design have increased the need for accurate measurement of shock and vibration. Consequently piezoelectric accelerometers have become very popular compared to traditional vibration transducers (velocity probes, eddy current probes, etc.), as they permit full utilization of the wide dynamic and frequency range and high resolution of the advanced measurement and analysis equipment of today.

The exterior design of the piezoelectric accelerometer has proved to be very efficient and as a consequence there have been no recent significant modifications. For general-purpose measurements the piezoelectric accelerometer has a metal housing with a microdot connector or an integral cable. For efficient mounting of the base most types are equipped with a 10–32 UNF threaded hole.

Thus, from the outside most piezoelectric accelerometers look very similar no matter when they were designed, or by which manufacturer. In spite of this, piezoelectric accelerometers cannot be considered standardized products with equally good or bad performance characteristics. This article focuses on how changes in the design of the sensing element, introduced by some manufacturers during recent years, have led to vast improvements in the performance of these accelerometers compared to the traditional designs.

In accordance with ISO and ANSI standards, the environmental parameters for a piezoelectric accelerometer are quantified from the respective time signals without specifying their frequency content.

In practical measuring situations, temperature transients and base bending are the environmental effects which most often cause problems. This paper describes measurements of these effects for different accelerometer designs. A Brüel & Kjær Dual Channel Signal Analyzer Type 2032/34 was used to quantify the environmental effects in the time and frequency domain.

Accelerometer Design

In general, a piezoelectric accelerometer can be considered as being a simple spring-mass system. The piezoelectric material acts as a linear spring with a high elastic constant which gives a wide, flat frequency range and a correspondingly wide, flat phase response (see Fig. 1).

While the mechanical properties of the accelerometer described above are governed by the elastic properties of the piezoelectric elements, the

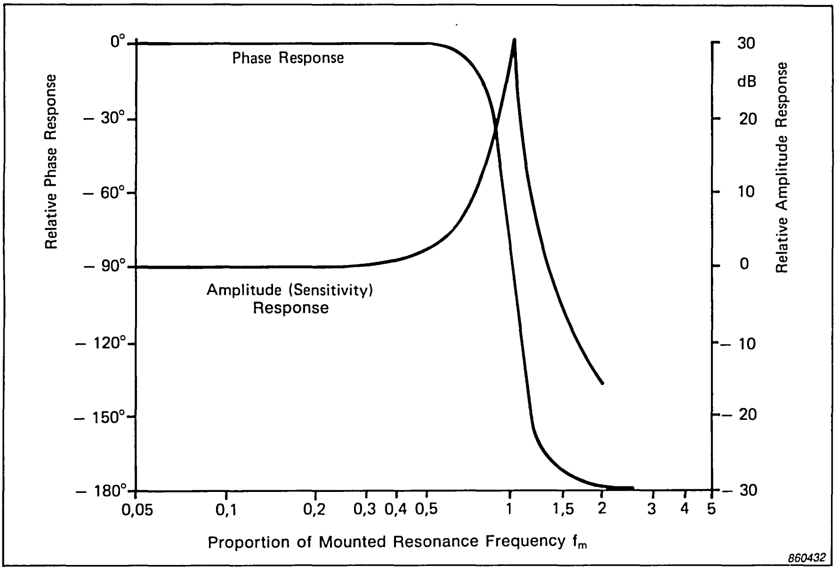

Fig. 1. Frequency and Phase response of a Brüel & Kjær piezoelectric accelerometer

electrical output is determined by the piezoelectric characteristics of these elements.

As indicated in Fig. 2, there are some electrically charged aligned domains inside the piezoelectric ceramic material. When shear or compression forces are applied to piezoelectric elements over a very wide dynamic range (160 dB), they generate a charge on the surfaces perpendicular to the polarization direction. The charge generated is proportional to the force applied, and therefore also (in the flat frequency response range of the accelerometer) proportional to the acceleration applied to the base of the accelerometer.

Design Considerations

For many years, several stable piezoelectric materials with highly linear mechanical and electrical properties have been known. The main effort in optimizing the performance of the piezoelectric accelerometer has therefore been devoted to the designing of a configuration of the spring mass system which gives an optimal utilization of the mechanical and electrical properties of these piezoelectric materials.

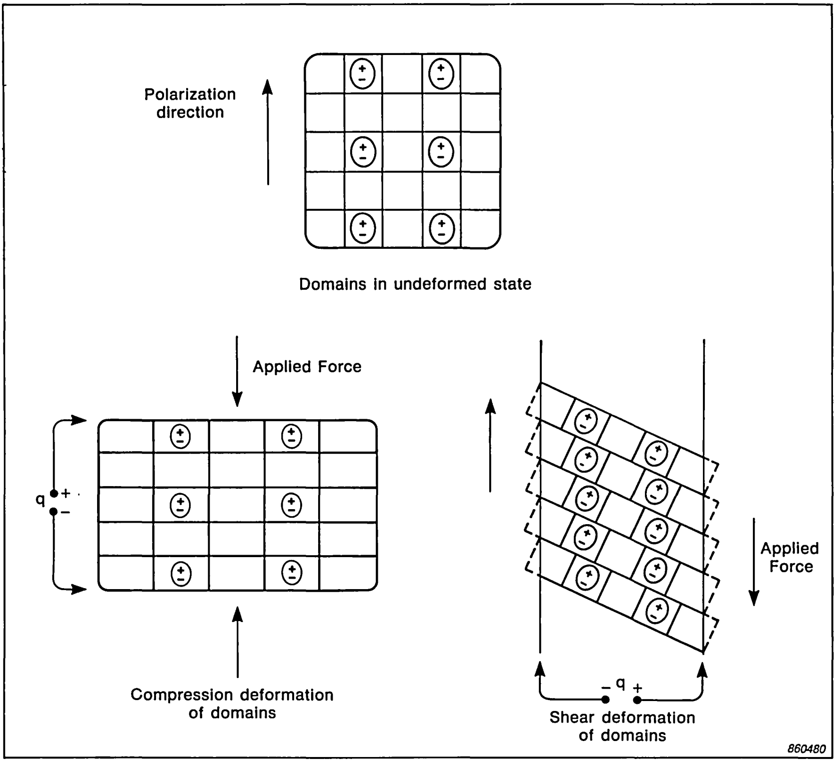

Fig. 2. Working principle of piezoelectric elements

As described in Ref. [1] the development in the mechanical design of the spring mass system has focused on

- how the piezoelectric element can be insulated from interaction with vibration-related forces other than the desired vibrational force
- how undesired signals from the piezoelectric element due to non-vibrational environmental influences can be prevented.

Normally the most serious environmental influences comes from **base bending** and from **temperature transients**. In the following the accelerometer designs shown in Fig. 3, which represent almost 100% of all piezoelectric accelerometers on the market today, will be used to illustrate

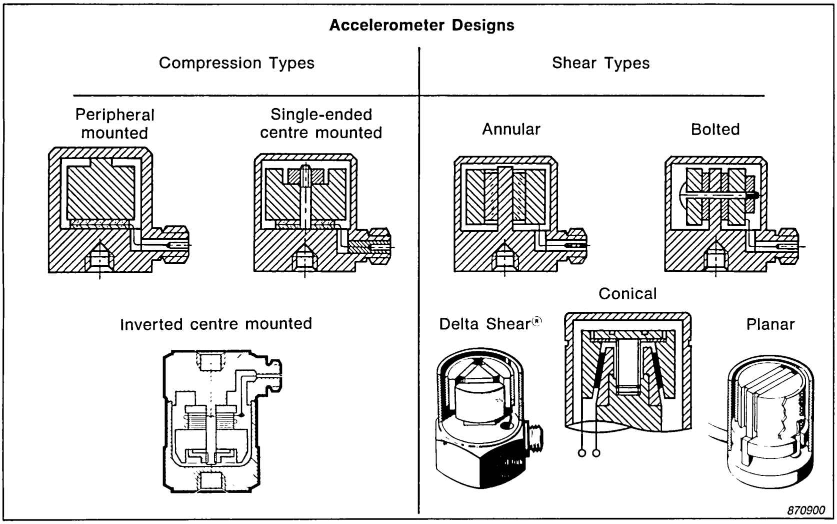

Fig. 3. Compression and Shear Type accelerometers

how the mechanical design of the sensing element influences the performance of the accelerometer. Depending on the way the piezoelectric elements are loaded, the accelerometers are characterized as **shear type** or **compression type** accelerometers. The measurements on temperature-transient and base-bending effects discussed in this paper are made on the following accelerometer designs: single-ended compression, bolted shear, conical shear, annular shear and the Brüel & Kjær Delta Shear®.

Base Bending

Designing against Base Bending

When vibration is present, so too is bending of the vibrating surface. Provided that the accelerometer is properly mounted, the bending will be transmitted to the accelerometer base.

As the output of the piezoelectric accelerometer is related to the force sensitivity of the piezoelectric material, the mechanical design of the spring mass system should employ an efficient way of transmitting the vibrational forces.

The traditional compression designs shown in Fig. 3 have this feature.

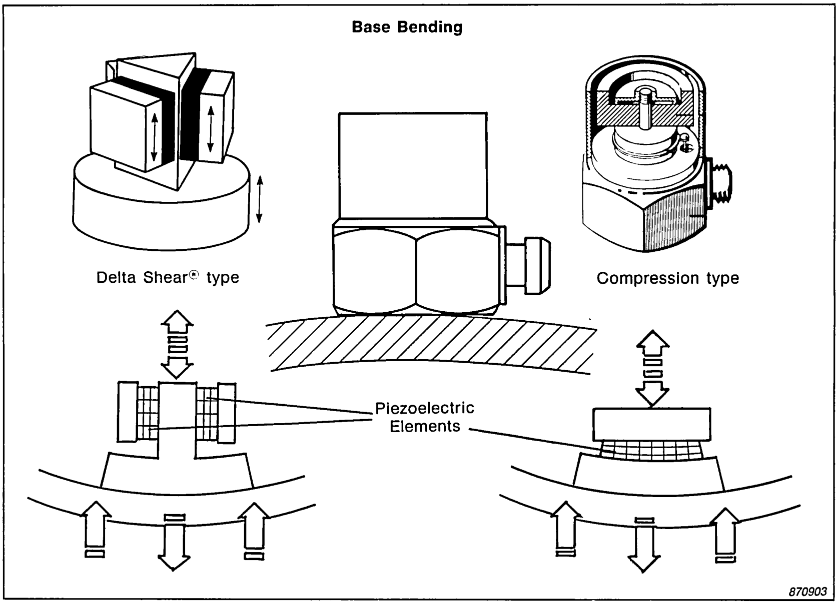

Fig. 4. Sensitivity of Shear and Compression type accelerometer to Base Bending

However, a very serious drawback of the compression designs is that they do not mechanically insulate the piezoelectric element from non-vibration-related forces.

For that reason the peripheral mounted compression design, where acoustical pressure acting on the housing will generate a non-vibration related output as the pressure is transmitted directly to the piezoelectric element, was given up long ago in favour of the single-ended centre-mounted compression design. Due to the fact that the single-ended compression design in its basic configuration is simple and inexpensive to make, probably more than 75% of all piezoelectric accelerometers made today are still of this design.

In a normal environment with stable temperature the dominating non-vibration-related forces will be the bending forces transmitted at the vibration frequency from the vibrating structure to the base of the accelerometer. Unfortunately, as shown in Fig. 4, these bending forces, which are always present, act directly on the piezoelectric element in the single-ended compression design, and thus cause an undesired output which adds to the vibrational output of the accelerometer.

Even when inserting a beryllium disc with high bending stiffness between the base and the piezoelectric element, the bending forces still cause undesired output. For that reason some years ago Brüel & Kjær and other manufacturers started to design piezoelectric accelerometers where the piezoelectric elements are exposed to shear forces instead of compression forces. Fig. 3 shows the most important shear designs used today. The Delta Shear® and the Planar Shear are the unique Brüel & Kjær designs.

Shear Type accelerometers generally have a much better performance than compression type accelerometers, as the piezoelectric elements are mechanically insulated from the base. This is illustrated in Fig.4.

Compared to other shear designs, the Delta Shear® and Planar Shear accelerometers seem to have the advantage that they employ two or three mechanically decoupled piezoelectric elements. Thus the "annular" and "conical" shear accelerometers seem to be rather sensitive to base bending due to the closed ring shape of their piezoelectric elements. Likewise, some "bolted" shear accelerometers are also sensitive to base bending. This is probably because the electrical insulation around the bolt holding the assembly together gives too stiff a coupling between the centre post pin and the masses.

Base Bending Test Results

The standard method for measurements of base strain sensitivity (described in ISO 5347 and ANSI S 2.11-1969 and originally in ANSI Z 24.21–1957) is to use a steel beam with dimensions of $3'' \times 0{,}5'' \times 57''$ or $76 \times 12{,}5 \times 1240\ \mathrm{mm}^3$ clamped at one end. The accelerometer under test and a set of strain-gauges are placed at a distance of $1{,}5''$ or 40 mm from the clamp. The beam is excited by hand. At a strain level of 250 $\mu\epsilon$ peak, the corresponding peak output from the accelerometer is measured.

An improved method was used to obtain more detailed information. The excitation was applied by a Brüel & Kjær Vibration Exciter Type 4805/4814 driven by a Brüel & Kjær Frequency Analyzer Type 2032/34. This was also used to analyze the outputs from the transducers and the strain-gauges. Examples of the outputs are shown in Figs. 5, 6 and 7.

A number of measurements at strain levels from 10 $\mu\epsilon$ to 250 $\mu\epsilon$ were made to investigate the harmonic content of the signals and the linearity of the Delta Shear® accelerometer Type 4371, with respect to this type of excitation.

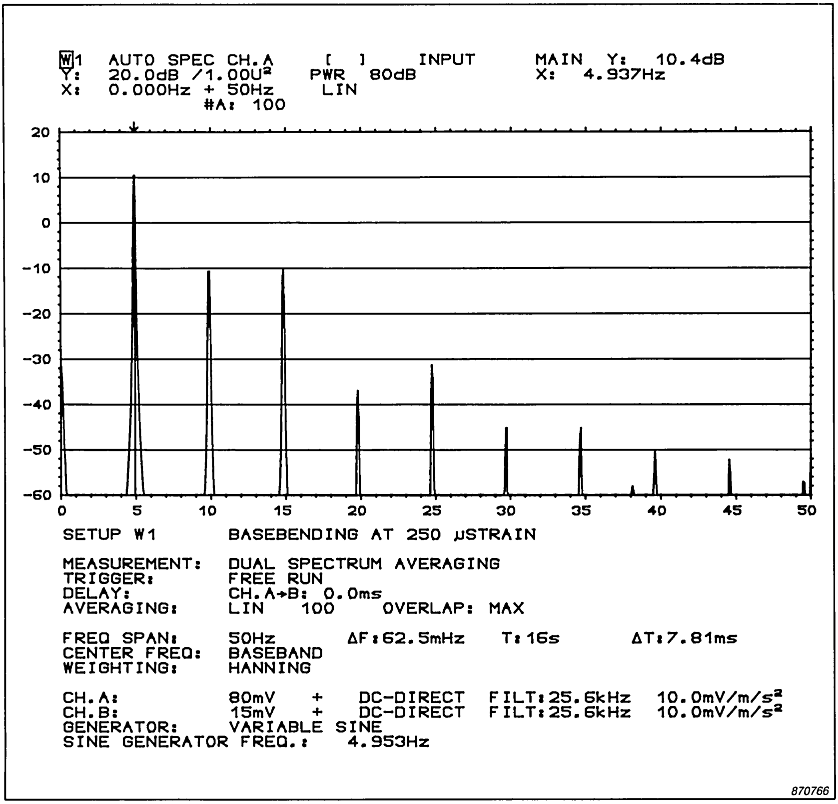

Fig. 5. Base Bending output signal from Brüel & Kjær Type 4371 Delta Shear® Accelerometer at 250 $\mu\epsilon$. Frequency range 0–50 Hz

The results are shown in Fig. 8 as the change in dB of the ratios between the accelerometer output and the strain input taken at the excitation frequency and at the 3^{rd} harmonic.

It is seen that a reasonably good linearity exists up to about $100\mu\epsilon$, but then the transducer signal starts to be distorted, which gives lower output at the excitation frequency and higher distortion.

This example shows that perhaps the choice of 250 $\mu\epsilon$ peak as the proper excitation level does not always lead to useful results, especially because strains of that magnitude do not normally occur.

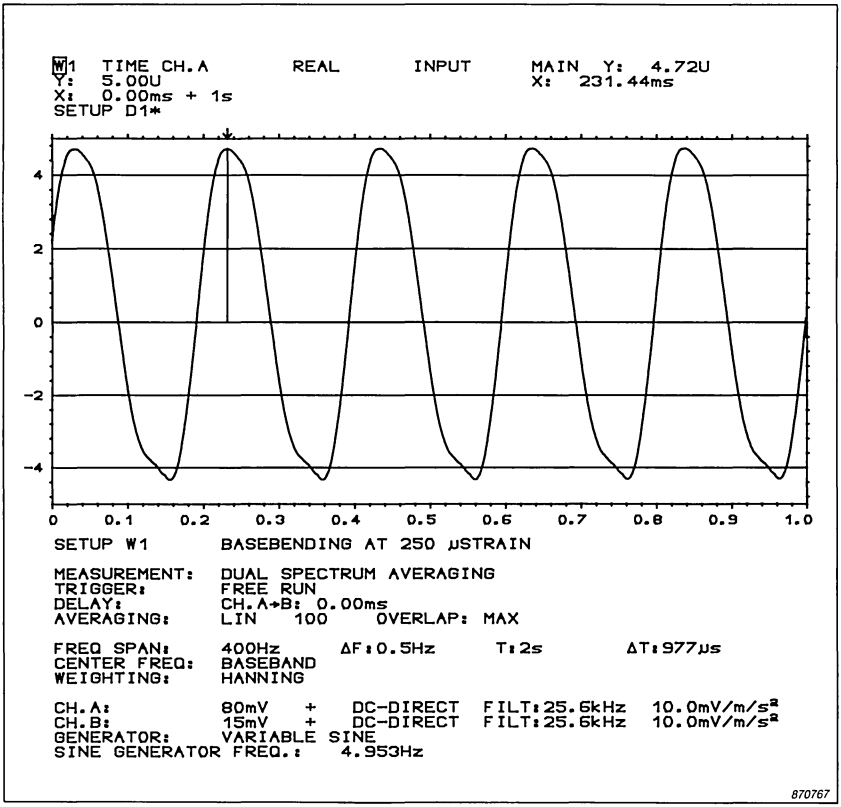

Fig. 6. Base Bending output signal from Brüel & Kjær Type 4371 Delta Shear® Accelerometer at 250 $\mu\epsilon$ 1 second time record

Furthermore the sensitivity at the third harmonic seems to be twice the sensitivity at the fundamental frequency of 4,75 Hz, i.e. the 3rd harmonic generated in the transducer is always bigger than the signal generated from strain at this frequency.

A number of different transducer designs were tested. An old Brüel & Kjær compression type was found to be more than 40 dB (100 times) more sensitive than the Delta Shear® accelerometer Type 4371.

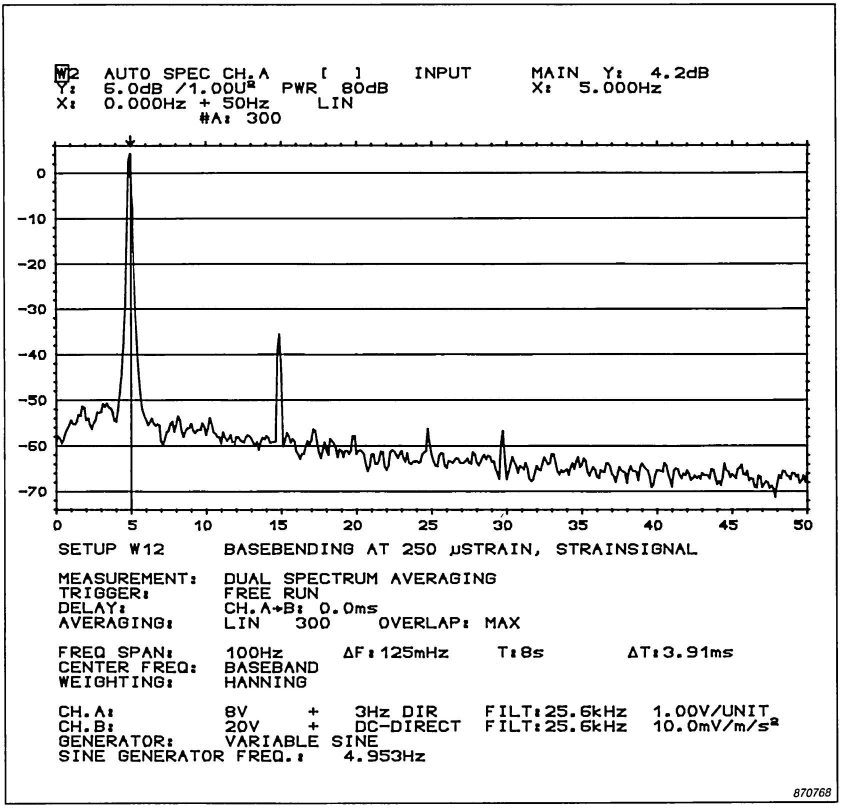

Fig. 7. Strain gauge output at 250 $\mu\epsilon$ on base strain beam. Frequency range 0–50 Hz

Different commonly used compression designs and some bolted, conical and annular shear types were tested. Base strain output levels 18 dB (8 times) to 33 dB (45 times) higher than the output from Type 4371 were found – which underline the superiority of the Delta Shear® design.

Temperature Transients

Designing against Temperature Transient Effects

Piezoelectric materials can be divided into three groups: monocrystalline materials (e.g. quartz), polycrystalline aggregates (e.g. ferroelectric ceramics) and polymeric substances (e.g. polyvinylidene flouride – PVDF).

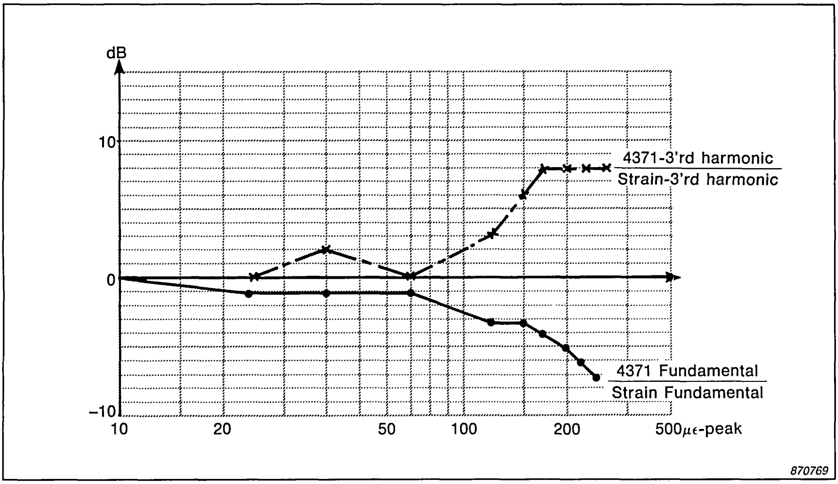

Fig. 8. Brüel & Kjær Type 4371 Delta Shear® Accelerometer output linearity for base strain 10–250 $\mu\epsilon$

For measurement transducers, by far the most important materials are quartz from the first group and lead-zirconate-titanate ceramics from the second group. Polymeric substances are normally considered to be too unstable for measurement purposes.

When thermal outputs are considered, the important difference between the piezoelectric materials is whether they exhibit a spontaneous internal electrical polarization or not. All artificially polarized materials like the above mentioned ceramics and polymers have internal electrical polarization whereas quartz and a few other crystals do not.

A change in temperature will impose a change in the internal polarization, giving rise to a charge build-up on the surfaces perpendicular to the polarization direction. This is the so-called pyroelectric effect which is highly undesirable in accelerometers. Pyroelectric effects are normally divided into primary effects, which occur at constant strain and uniform temperature, secondary effects, which occur at constant stress and uniform temperature and finally tertiary pyroelectric effects which arise in all piezoelectric materials due to temperature gradients across the piezoelectric element.

This could lead to the conclusion that quartz would be ideal, but its very low charge sensitivity (approx. 200 times less than ceramics) and the fact

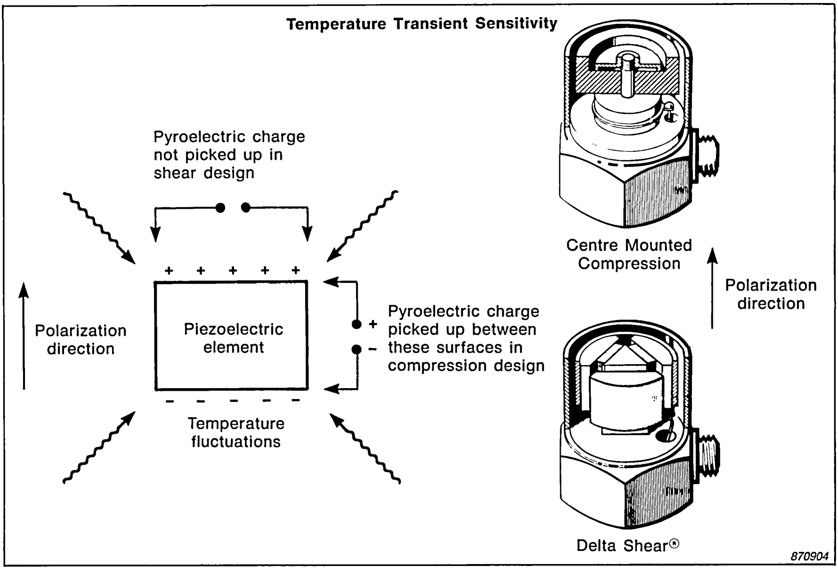

Fig. 9. Sensitivity of Shear and Compression type accelerometer to temperature transients

that ceramics can easily be made into any shape desired, whereas quartz has to be ground into the right shape from an artificially or naturally grown crystal, make ceramics by far the most commonly used material.

Using the shear configuration removes the signals caused by the primary and secondary pyroelectric effects, as illustrated in Fig. 9, as the surfaces from which the signals are picked up are parallel to the polarization direction and therefore do not give output signals due to these effects.

Therefore the mechanical shear configuration also has the advantage that very sensitive piezoelectric ceramic materials can be used. Furthermore, the necessary preloading in the shear configuration also acts in a direction perpendicular to the sensitive axis in contrast to the compression configuration.

In many compression types still produced, the piezoelectric elements are often, for the above-mentioned reason, made of quartz. In spite of this, due to forces from thermal expansion/contraction in the preloading mechanical system, they are still very sensitive to temperature transient effects. Furthermore, these compression type accelerometers often have a degra-

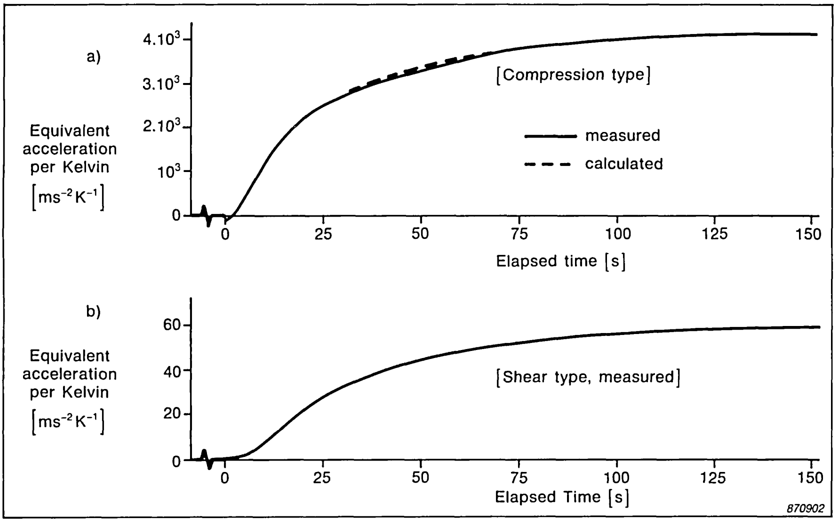

Fig. 10. Equivalent acceleration resulting from the pyroelectric response to a temperature step of +25°K produced by total submersion in water of an unmounted accelerometer
a) compression type (Brüel & Kjær 4332)
b) Shear Type (Brüel & Kjær 4366)

ded performance due to the built-in electronics employed to compensate for the low charge sensitivity of the quartz elements.

In Ref. [2] different accelerometers have been modelled. If charge amplifiers with very long time constants (nearly DC response) are used, results, as shown in Fig. 10, will be found from models and experiments, illustrating the large reduction in the primary and secondary pyroelectric effects obtained by the shear configuration (approximately 100 times).

Furthermore, the initial slope on the curves interacts with the lower limiting frequency of the preamplifier used, increasing the advantage of the shear configuration as shown in Fig. 11, giving a difference of 2000 times.

Temperature Transient Test Results

Three methods were used to measure the temperature transient sensitivity of the accelerometers under test.

A test method where the test accelerometer base is mounted on a heating element was employed to simulate effects from temperature changes of

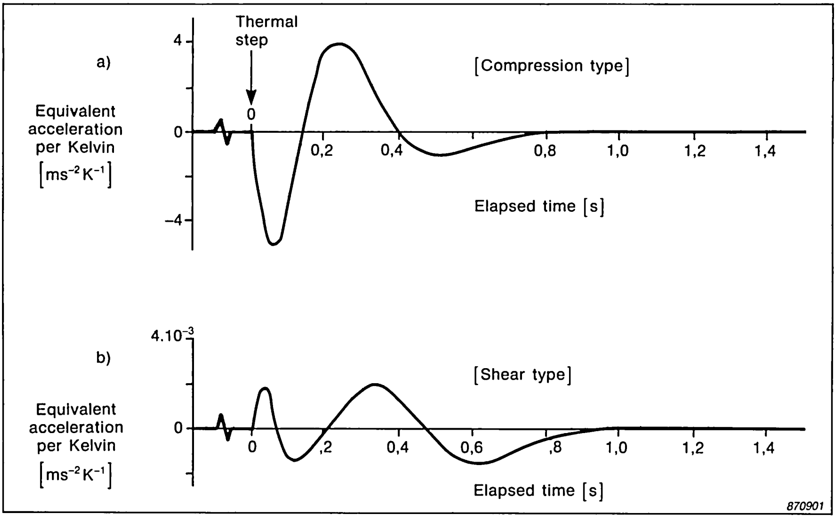

Fig. 11. Equivalent acceleration produced by a positive temperature step, measured with a charge amplifier with a third-order Butterworth high-pass characteristic and a 3 Hz – lower cut-off frequency

a structure (the ambient temperature being constant). To simulate how an accelerometer responds to changes in the ambient temperature, the test accelerometer was mounted on a 5 kg aluminium block and hot air was blown on the accelerometer. The third method employed followed the guidelines given in ISO 5347. Here the accelerometer was mounted on an aluminium block. The block and transducer were then immersed in water with a temperature of approximately 25°C above the ambient temperature.

The temperature transient effects were measured in the time and frequency domain with a Brüel & Kjær Dual Channel Signal Analyzer Type 2032/34. The settings on the Brüel & Kjær accelerometer preamplifier used were LLF: 0,2 Hz ULF: 0,1 kHz.

The transducers tested were a Brüel & Kjær Type 4371 Delta Shear® accelerometer, an earlier Brüel & Kjær compression type accelerometer together with various other compression designs and some bolted, conical and annular shear accelerometer designs made by other manufacturers.

In general, significant peaks in the frequency spectra from temperature transient effects are found in a range below 2 Hz.

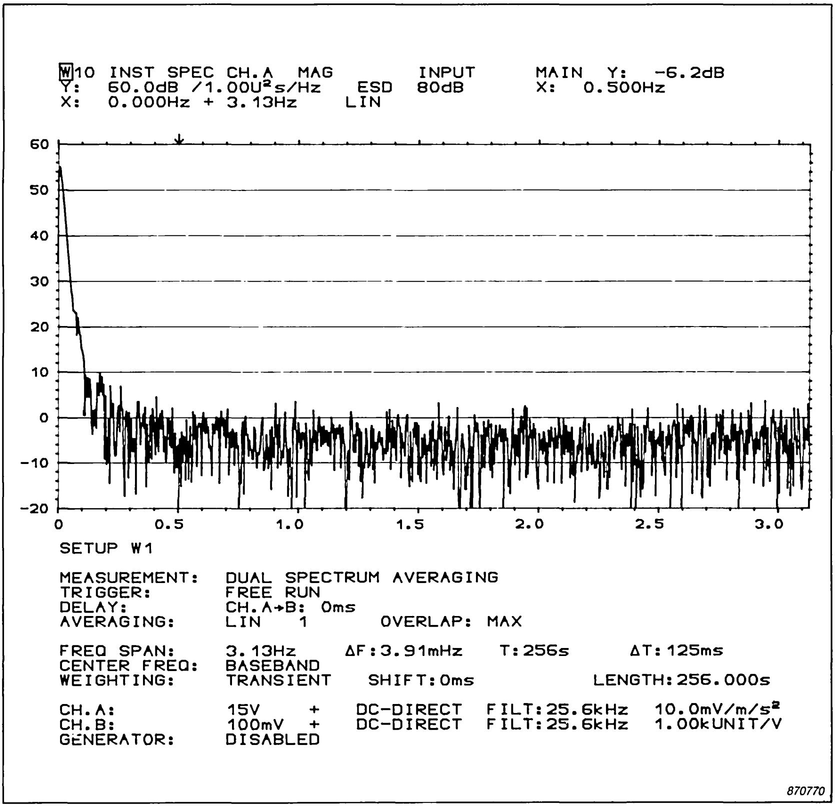

Fig. 12. Temperature-transient response for Brüel & Kjær Type 4371 Delta Shear® accelerometer, heating of base

In the case of temperature transient characteristics, the measurements also underlined the superiority of the Delta Shear® design. For the Delta Shear® design, the maximum output from the temperature transient, when the base of the accelerometer was heated was 60 dB above the noise while the level for all other accelerometers was 75 dB or more above the noise. (See Figs. 12, 13 and 14). Note that the gain has been reduced 20 dB in Figs. 13 and 14. This increases the noise level by 20 dB. As the components are at low frequencies, this implies in practice that when a Delta Shear® accelerometer is used, the lower limiting frequency limit on the preamplifier can be set a factor of approximately 10 times lower than when

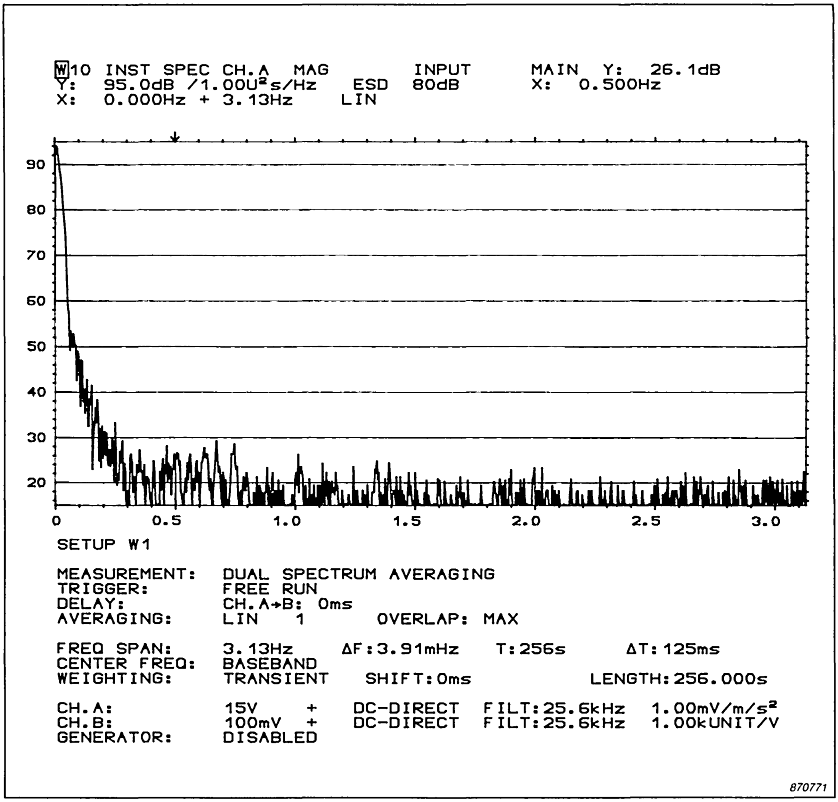

Fig. 13. Temperature-transient response for Brüel & Kjær Type 4343 Compression type accelerometer, heating of base

using other accelerometers without overloading the preamplifiers on account of temperature transients.

The measurements have demonstrated that for low-level measurements and especially for low-level low-frequency measurements, the effects from temperature transients must be considered a very important noise source. The only way to cope with the noise is to try to limit the temperature fluctuation or to use an accelerometer like the Delta Shear® which has a low sensitivity to temperature transients.

One of the designs under test, a line-drive compression type employing quartz as the piezoelectric element, showed a significant change in temperature transient sensitivity depending on how the transient was applied.

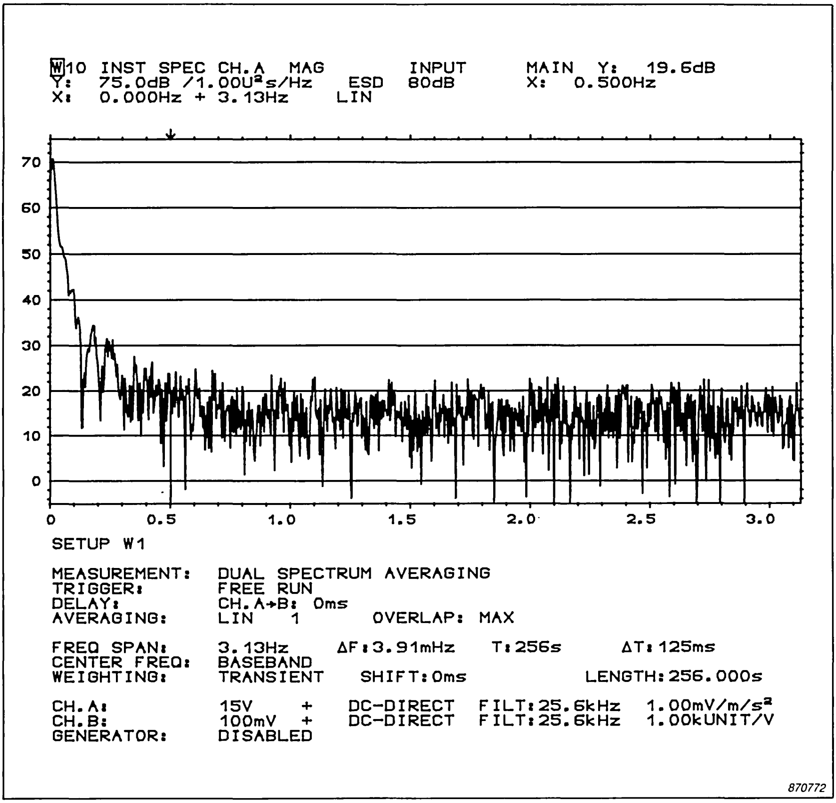

Fig. 14. Temperature-transient response for annular Shear accelerometer, heating of base

For this accelerometer Figs. 15 and 16 show a difference of 10 times between the peaks in the spectra obtained by 1) heating the base and 2) blowing hot air onto the housing. The same thermal inputs gave two nearly identical peaks in the spectra from the Brüel & Kjær Type 4371 Delta Shear® accelerometer shown in Figs. 17 and 18.

The published data given for this above-mentioned compression accelerometer seems to be obtained by only heating the base. Therefore, in practical use, where changes in the ambient temperature are the predominant form of exposure, it is likely that the measurement error will be bigger than expected from the manufacturer's specifications.

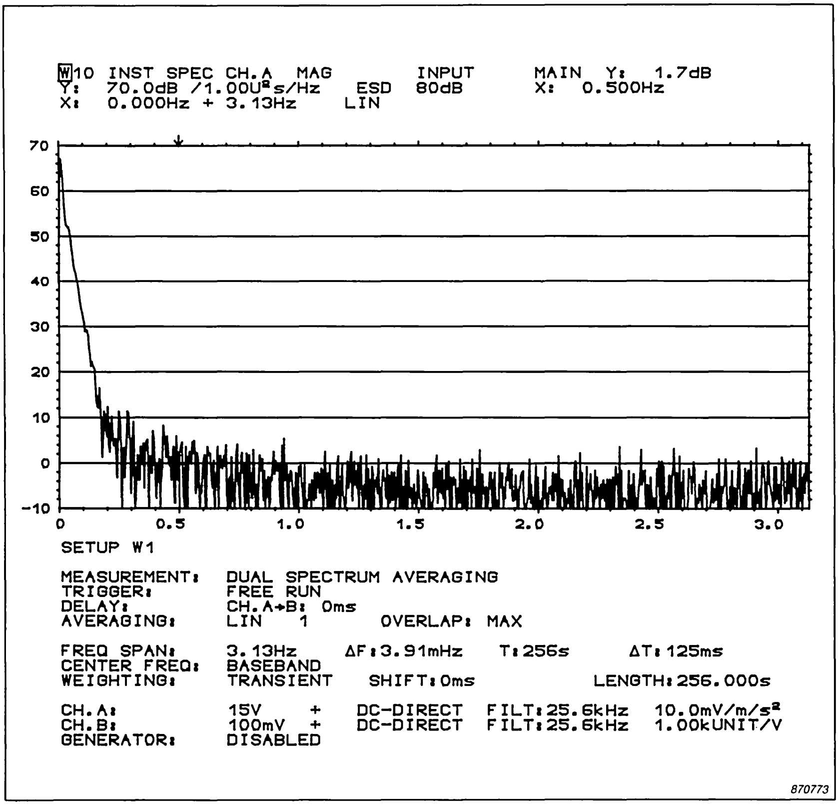

Fig. 15. Temperature-transient response of compression type accelerometer with built-in electronics, piezoelectric elements made of quartz, heating of base

The two spectra in Figs. 15 and 16 illustrate yet another aspect of the same problem. To avoid overloading of the preamplifier, the gain is reduced by a factor of 10 in Fig. 16, which gives a preamplifier noise floor corresponding to a ten times higher vibration. Thus, if very high cut-off frequencies cannot be used, a significant reduction in the capability of the transducers to measure low-level low-frequency signals is the result. This could not be predicted from the manufacturer's specifications.

ISO 5347 seems to give a good simulation of temperature transient effects as being a combined thermal exposure to base and housing.

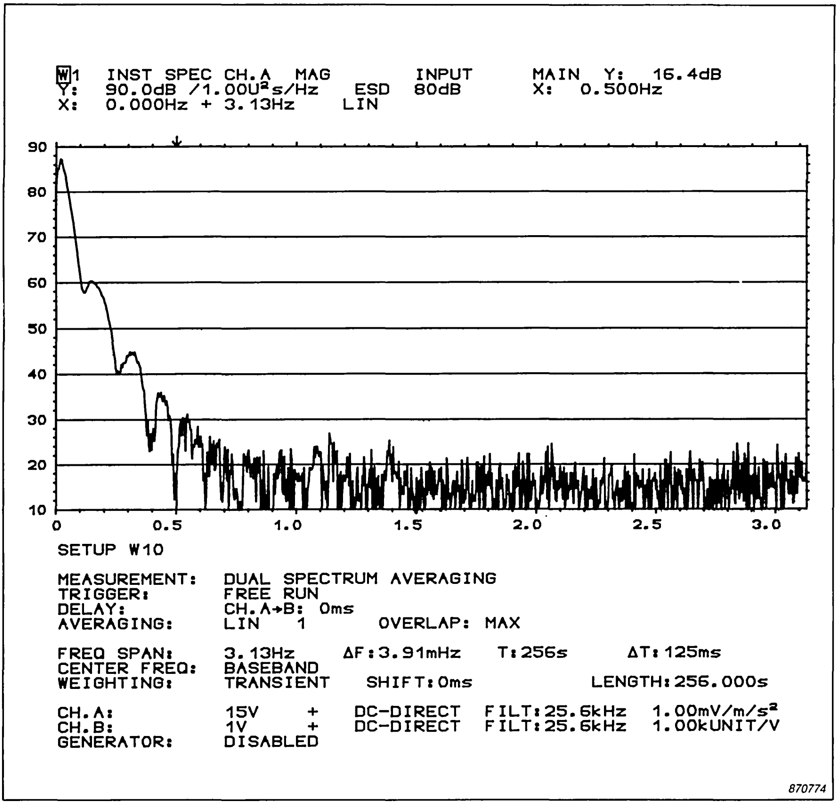

Fig. 16. Temperature-transient response of compression type accelerometer shown in Fig. 15. The only difference is that the temperature transient has been applied to the housing of the accelerometer

Other Design Considerations

A very important design consideration is the long-term stability and linearity of the accelerometer. Here, carefully made compression-type accelerometers, such as, for example, the Inverse Center Mounted Compression type used by most manufacturers as Standard Reference Accelerometers for Calibration and carefully made shear designs are equally good. If the accelerometer is not stable, it is hardly worth the effort spending time and money on a calibration by following one of the methods described in Ref. [3].

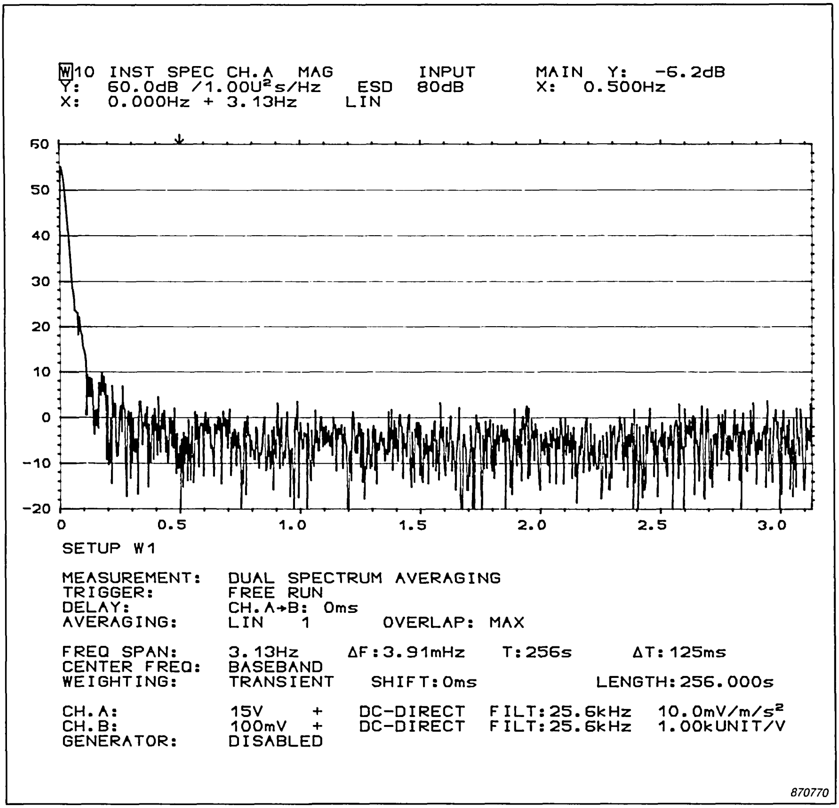

Fig. 17. Temperature transient response of Brüel & Kjær Type 4371 Delta Shear® accelerometer, heating of base

Conclusion

The measurements made demonstrated that a proper accelerometer design is of great importance if good vibration data is required.

Even though most piezoelectric accelerometers look the same, they do not have the same performance characteristics, due to different designs of the sensitive element. At least 75% of all piezoelectric general purpose accelerometers on the market today are of the single-ended compression design. These have a very poor performance compared to the shear designs. Among the shear designs available, the Brüel & Kjær accelerometers

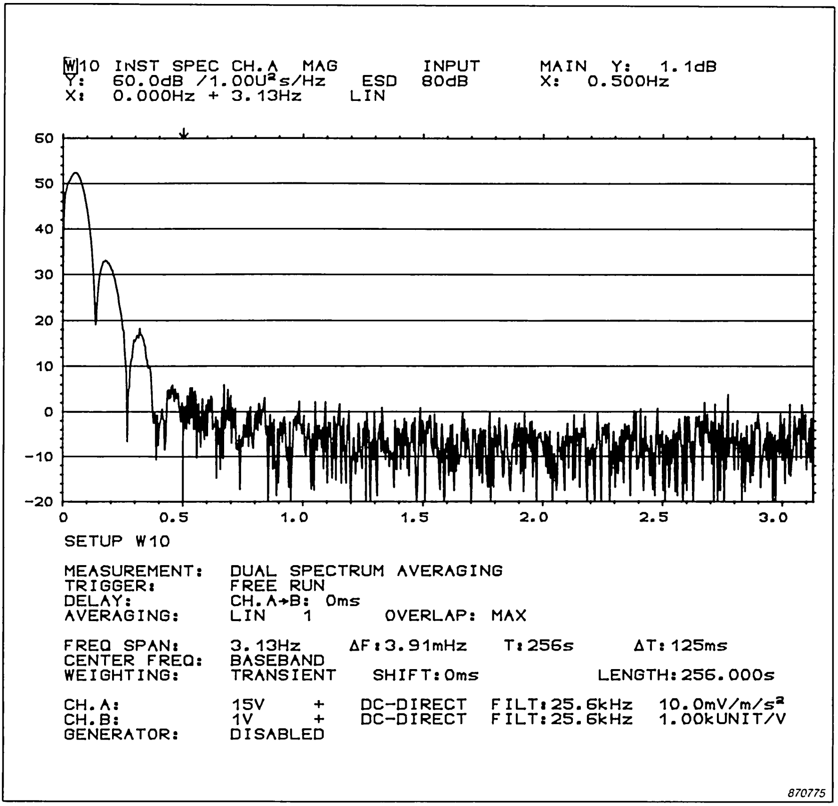

Fig. 18. Temperature transient response of Brüel & Kjær Type 4371 Delta Shear® accelerometer, heating of housing

have some superior design features which make them relatively less sensitive to base bending and temperature transients, and still very rugged and stable.

The measurements also demonstrated that a single value is generally not sufficient to give a proper evaluation of the sensitivity of a transducer to environmental effects. Not only the transducer time signal generated by the environmental exposure but also the frequency spectrum of this signal is necessary to reveal the overall behaviour of the transducer.

The measurements of base strain sensitivities in accordance with the standards indicated that measurements at lower strain levels give better information. Thus, at lower strain levels than prescribed in the standards, 3 times higher base-strain sensitivities were found. Furthermore, the harmonic content, only 10–20 dB lower than the fundamental at higher strain levels, is important information when possible sources of measurement errors are investigated.

The superiority of the Brüel & Kjær Delta Shear® Design compared to a number of other constructions is proved by improvements from 18 to 33 dB in the base-strain sensitivities.

Measurements on temperature transient effects showed that these are generally characterized as having a very high amplitude in the low frequency region from 0 to 2 Hz. The Brüel & Kjær Delta Shear® Accelerometer Type 4371 showed a peak level 15 dB lower than others when exposed to a temperature transient. This means that Brüel & Kjær, with this design, has extended the frequency range approximately one decade down compared to the other piezoelectric accelerometer designs.

The measurements also indicated that some designs, here a compression type accelerometer with built-in electronics, showed a significant variation of the sensitivity to temperature transients, depending on how the transient is applied. To ensure that the users are properly informed, the measurements made indicated that if the manufacturers follow the guidelines in ISO 5347, the data given will give a good estimate of the worst-case temperature-transient sensitivity.

References

[1] Serridge, M. & Licht, T. — *"Piezoelectric Accelerometers and Vibration Preamplifiers"*. Brüel & Kjær Handbook

[2] Klaassen, K. — *"Pyroelectric Side-Effects in Piezoelectric Accelerometers"* Conference Proceedings, SENSOR'82 Transducer Technology and Temperature Measurement. Jan. 1982

[3] Licht, T.R. & Andersen, H. — *"Trends in Accelerometer Calibration"*. Brüel & Kjær Technical Review No.2–1987

Trends in Accelerometer Calibration

by Torben R. Licht and Henrik Andersen

Abstract

This paper discusses the calibration accuracy and user-friendliness of accelerometer calibration using laser interferometry, traditional comparison calibration methods and FFT broad-band comparison calibration methods.

Sommaire

Dans cet article sont discutés la précision de l'étalonnage et la facilité d'utilisation de l'étalonnage d'accéléromètres par interférométrie laser, par comparaison, et par comparaison utilisant la technique de FFT large-bande.

Zusammenfassung

Die Genauigkeit und Anwenderfreundlichkeit der Kalibrierung von Beschleunigungsaufnehmern mittels Laserinterferometrie, herkömmlicher Vergleichsmethoden und der FFT- Breitband-Vergleichsmethode werden in diesem Artikel diskutiert.

Nomenclature

U_r	random uncertainty
U_s	systematic uncertainty
U_c	comparison uncertainty
U_t	total uncertainty
n	number of measurements
x_i	value of individual measurement
$\bar{x}$	sample mean value
s	standard deviation
σ (est)	standard deviation estimate
t	student t factor
K	normal distribution factor
a_i, e_i	semi-ranges for systematic uncertainty components
λ	wavelength of laser light
R_f	fringes per period
ω	angular frequency
X_o, X	displacement amplitudes
A_o, A	acceleration amplitudes
S	charge sensitivity
H	frequency response function

Introduction

Advances in the design of structures and machines over recent years have created more vibration problems. The need for accurate measurement of shock and vibration has become very important. Consequently, a lot of effort has been put into optimizing the design of vibration transducers and into specifying their calibration procedures.

This paper focuses on methods for the dynamic calibration of piezoelectric accelerometers. This type of vibration transducer has become very popular because of its high sensitivity-to-mass ratio and its low sensitivity to adverse environments. The piezoelectric accelerometer also has extremely wide frequency and dynamic ranges to match the performance of the advanced measuring and analysis equipment of today.

Calibration in general refers to the procedures used to verify all the performance characteristics which can influence the accuracy of measurements made by the transducer. Even though the performance characteristics are little affected or unaffected by time and extraneous environments, good instrumentation practice, and often legal obligations too, require the users of piezoelectric accelerometers to confirm the manufacturers' calibration and to recalibrate the transducers at fixed intervals of time.

Recalibration of piezoelectric accelerometers is usually understood to be recalibration of the main axis sensitivity at a specific frequency, combined with a frequency response measurement to check the overall state of the transducer.

In accordance with this, the present paper focuses on the trends in the methods used for sensitivity calibration and frequency response measurements of piezoelectric accelerometers.

The paper will discuss absolute calibration by using laser interferometry and two comparison calibration methods, one using sine excitation and one using random excitation. The methods are compared with regard to calibration accuracy and user-friendliness.

Classification of Calibration Methods

The main axis sensitivity is determined either by absolute calibration or comparison calibration.

Absolute Calibration implies that the accelerometer sensitivity is determined by measurements based on fundamental and derived units for the physical quantities involved.

Today the most convenient method for absolute calibration is laser interferometry. Thus, since the advent of the laser, reciprocity calibration is becoming rare as this method is rather involved and requires very careful measurements to obtain good results.

Comparison Calibration implies that the sensitivity of the transducer to be calibrated is measured relative to a Standard Reference Transducer with known sensitivity.

Compared to the absolute laser interferometer calibration, comparison calibration is simpler to perform and requires less complex and expensive instruments. Therefore comparison calibration is a very attractive calibration method for average users of accelerometers while the absolute method typically is applied by International and National Standard Institutes and major calibration laboratories in industry.

The calibration accuracy will of course depend on the method used. As comparison calibration requires the use of an absolute calibrated accelerometer, the accuracy of the comparison calibration will, in all cases, be less than the calibration accuracy of the Standard Reference Transducer used.

International Calibration Hierarchy; Traceability

To avoid the necessity of carrying out absolute calibrations of all accelerometers for common use, a hierarchy of Standard Transducers, accelerometers used for calibration, is established.

As shown in Fig. 1 the Standard Transducers are ranked in three groups

Primary Standard Transducers are calibrated by absolute methods. They are kept at the International and National Standard Institutes or at the Calibration Laboratories where they have been calibrated.

Transfer Standard Transducers are calibrated by comparison or absolute methods at the above-mentioned Institutes and Laboratories.

By interchanging and recalibrating Transfer Standard Transducers among International and National Standard Institutes, consistency is established.

By interchanging and recalibrating Transfer Standard Transducers between a Standard Institute and various Calibration Laboratories the con-

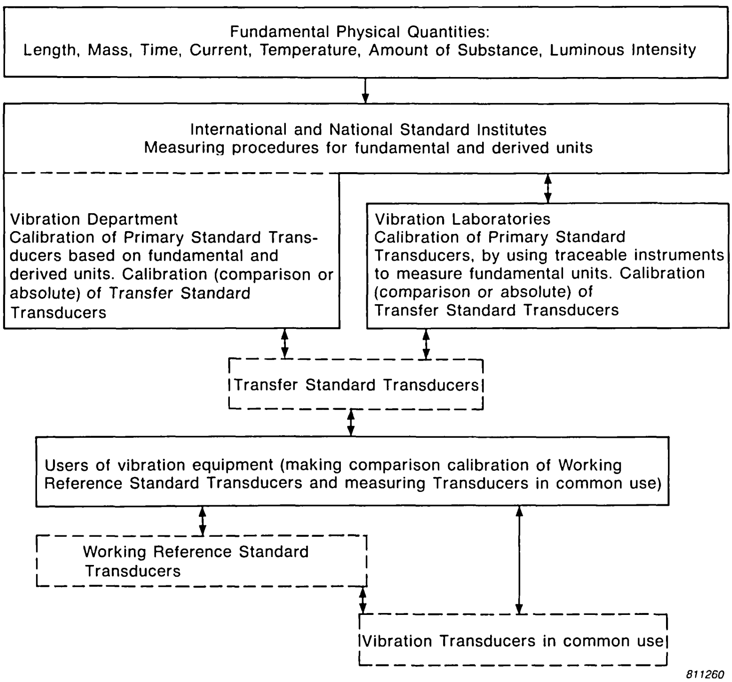

Fig. 1. Calibration hierarchy

sistency of the calibration they carry out is established. To keep track of which Standard Institute or Institutes have established the consistency of the calibration performed at a particular Calibration Laboratory, the transducers calibrated there are designated to be traceable to the Standard Institute/Institutes.

Working Reference Standard Transducers are used for comparison calibration of accelerometers in common use, i.e. actual measurements.

Working Reference Standard Transducers are calibrated by Standard Institutes or Calibration Laboratories by using absolute or comparison calibration methods.

The Working Reference Standard Transducers are checked by means of Transfer Standard Transducers. In this way the consistency and hence the traceability of the calibration of Vibration Transducers in common use are ensured.

Calibration Uncertainty

It is important to note that traceability only implies consistency with calibration performed at the Standard Institute /Institutes referred to, and thus only that the calibration is within tolerances.

This means that if a Calibration Laboratory is using more accurate instruments or a more sophisticated calibration set-up than the one used at the Standard Institute it refers to through the traceability, the uncertainty of the calibration performed by the Calibration Laboratory will be less than the uncertainty of the calibration performed by the Standard Institute.

In order to evaluate the accuracy of various calibration methods, the uncertainty of the calibration must be treated in a consistent way. In this paper the method described in the British Calibration Service Guidance Publication B 3003 [1] will be used.

The publication outlines a method for assigning a single ($\pm$) value of uncertainty for the measurement, including a statement of confidence in terms of the probability that the true value for the measurement lies between the ($\pm$) limits stated.

The contributions to the calibration uncertainty are, for practical convenience, classified as either random or systematic components.

The **Random Uncertainty** (U_r) appears as variations in the results when a measurement is performed a number of times under substantially the same conditions. The small independent random variables causing these variations are quantified as the random uncertainty of the measurement.

By repeating the measurement a large number of times n, the mean values for the arithmetic means $\bar{x}$ and the standard deviations s of the samples will usually approach a Gaussian probability distribution describing the distribution of all possible results of repeated measurements.

By using a limited number of measurements, an estimate σ (est) for the standard deviation of the probability distribution for the whole population can be found from the relationship

$$\sigma^2 \,(\text{est}) = \frac{1}{(n-1)} \sum_{1}^{n} (x_i - \bar{x})^2 \tag{1}$$

where x_i is the value of the individual measurements and $\bar{x}$ is their mean value.

The random uncertainty limit ($\pm\ U_r$) about the sample mean $\bar{x}$ that will embrace the population mean can, for a given Confidence Level, CL be calculated from σ (est) as

$$U_r = t \left[\frac{\sigma\,(\text{est})}{\sqrt{n}} \right] \tag{2}$$

where t is the student's t factor corresponding to the number of measurements used to estimate σ (est), and the chosen Confidence Level and n is the number of measurements made.

The **Systematic Uncertainty** (U_s) is made up of components which have constant, but not exactly known, values during the measurements.

The components contributing to the systematic uncertainty come from calibration factors, measuring apparatus, operational procedures and items under test.

Often the knowledge of the nature of the contributions will be so limited that a rectangular probability distribution, in the range of the limits $\pm\ a_i$ assigned, must be assumed.

When a number of distributions of whatever form are combined, the probability density distribution will approach the Gaussian Form. By using the semi-ranges a_i for the limits assigned, the systematic uncertainty limit ($\pm\ U_s$) about the sample mean $\bar{x}$ that will embrace the population mean can be calculated as

$$U_s = \frac{K}{\sqrt{3}} \sqrt{\sum_{1}^{n} a_i^2} \tag{3}$$

where K is the normal distribution factor corresponding to the specified Confidence Level.

The **Single Value of Total Uncertainty** is given by

$$U_t = \sqrt{U_r^2 + U_s^2} \tag{4}$$

and the result of the calibration is reported as

$$\bar{x} \pm U_t \tag{5}$$

accompanied by the statement of the Confidence Level of the estimate.

Calibration by Laser Interferometry

A typical set-up for this type of calibration is shown in Fig. 2. The principles used have been described in various papers [2, 3, 4, 5, 6] and are included in ISO 5347. All are based on the extremely stable and well-known wavelength λ of the laser light.

Three different methods are used to obtain information from the readout of the photo-diode in the Michelson interferometer. The simplest method is used at frequencies up to about 1000 Hz. It is based on counting the number of intensity changes R_f per vibration period (also referred to as "fringe counting").

It can easily be shown that the displacement amplitude of the vibration is given by

$$X_o = R_f \cdot \frac{\lambda}{8} \tag{6}$$

For a sinusoidal vibration at the angular frequency ω for which the displacement is described as

$$X = X_o \sin \omega t \tag{7}$$

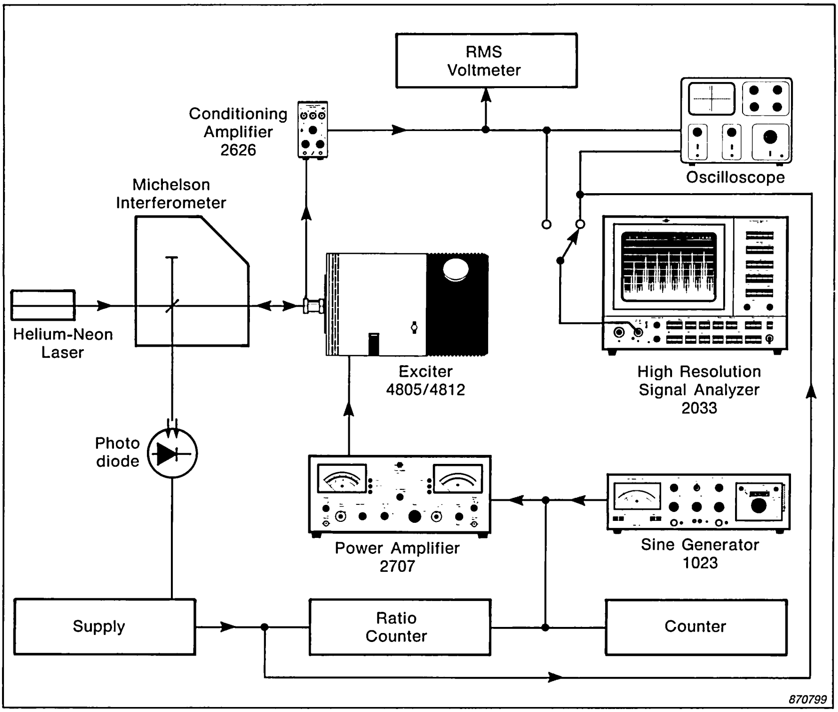

Fig. 2. Laser calibration set-up

the acceleration is given by

$$A = -\omega^2 X_o \sin \omega t = -A_o \sin \omega t \tag{8}$$

giving the result for the acceleration amplitude

$$A_o = \omega^2 X_o = \omega^2 \cdot R_f \cdot \frac{\lambda}{8} \tag{9}$$

From this it is clear that we have to consider the uncertainties of the fringe counting and the vibration frequency. From the set-up it is seen that uncertainties of voltmeter and charge amplifier must be taken into account, and finally we know that tilting of the transducer during the vibra-

e_1	Voltmeter + Charge Ampl.	± 0,08 %
e_2	Counter × 2	± 0,002 %
e_3	Fringe Counting (R_f)	± 0,02 %
e_4	Distortion	± 0,1 %
e_5	Tilting	± 0,2 %
e_6	Temperature	± 0,1 %
e_7	Transverse Vibration (max. 5%)	± 0,1 %
σ	Estimated standard deviation (from 3 measurements)	± 0,02 %

T01369GB1

Table 1. Laser calibration uncertainties at 160 Hz on a B & K Standard Reference Transducer Type 8305

tion cycle, together with transverse vibration, distortion of the sinusoidal movement and temperature, can create errors which must be evaluated.

The estimated errors from a measurement at 160 Hz on a Brüel & Kjær Standard Reference Transducer Type 8305 are given in Table 1.

The random error for a 99% Confidence Level is found from (2) by using $n = 3$, $t = 9,92$ and σ from the last line in the table.

$$U_r = 0{,}12\% \qquad (10)$$

The systematic error is found from (3) using the values in the table and $K = 2,58$ (99% CL):

$$U_s = \frac{2{,}58}{\sqrt{3}} \sqrt{e_1^2 + e_2^2 + e_3^2 + e_4^2 + e_5^2 + e_6^2 + e_7^2} = 0{,}42\% \qquad (11)$$

This leads to the total uncertainty

$$U = \sqrt{U_r^2 + U_s^2} = 0{,}44\% \qquad (12)$$

International "Round Robin" calibrations have demonstrated that uncertainties calculated according to these principles are in good agreement with the observed deviations and do not indicate that more conservative methods like direct additive calculation of uncertainties can be justified.

Comparison Calibration Methods

Back-to-Back calibration is performed by subjecting two accelerometers to the same sinusoidal vibration and comparing their outputs. The sensitivity of one accelerometer can be found if the sensitivity of the other is wellknown.

Simple Back-to-Back Comparison Calibration Method

A set-up for simple comparison calibration is shown in Fig. 3. The Brüel & Kjær Sensitivity Comparator Type 2970 is basically a summation amplifier but simpler systems using a selector and a voltmeter are sometimes employed.

The system can be balanced initially by applying the same charge input to both channels (by means of a generator and two matched capacitors).

Afterwards the sensitivity of the unknown accelerometer is found by changing the settings on the Precision Conditioning Amplifier. When a minimum is found on the comparator, the accelerometer sensitivity can be read off the Precision Conditioning Amplifier.

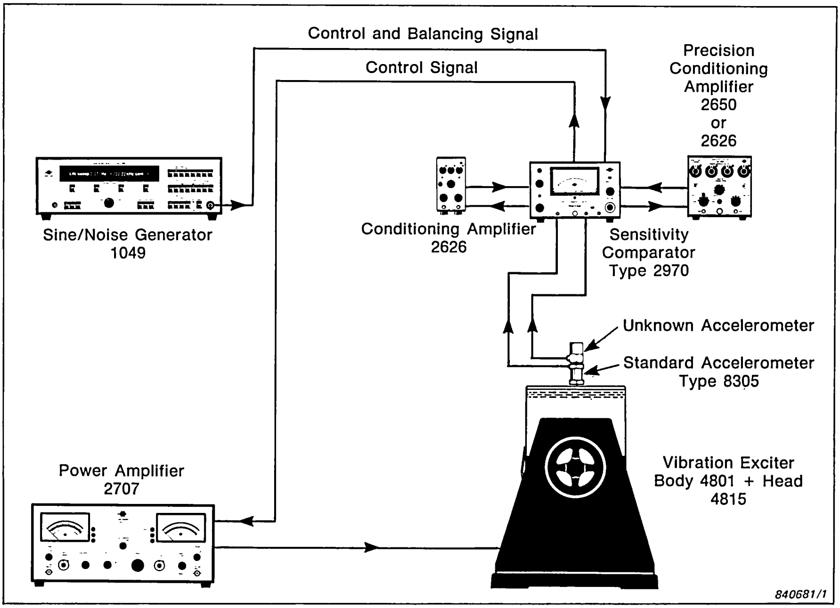

Fig. 3. Simple comparison calibration set-up

e_1	Variation of output from 8305 due to transverse component of vibration (max 3%)	± 0,06%
e_2	Transverse component from test accelerometer	± 0,15%
e_3	Sensitivity error of 8305 due to a temperature variation of ± 3°C from original calibration temperature	± 0,1%
e_4	Sensitivity variation of test accelerometer due to ± 3°C temperature variation	± 0,3%
e_5	Error in setting sensitivity controls on 2650	± 0,1%
e_6	Error in balancing the two amplifier inputs via 2970 balance control	± 0,3%
e_7	Calibration uncertainty of 8305 (at 99% CL)	± 0,6%
σ	Estimated standard deviation (10 measurements)	± 0,13

T01370GB1

Table 2. Uncertainties for simple back-to-back calibration at 160 Hz

Table 2 shows the uncertainties in the system.
From (3) the systematic error is:

$$U_s = \frac{K}{\sqrt{3}} \sqrt{e_1^2 + e_2^2 + e_3^2 + e_4^2 + e_6^2} \tag{13}$$

at a Confidence Level of 99% K is given as 2,58 giving

$$U_s = 0{,}71\% \tag{14}$$

The standard deviation listed in the table is obtained by means of 10 measurements. We know that $t = 3{,}25$ at a Confidence Level of 99%. Therefore, when only one measurement is made, we use the earlier experience for σ(est) and get the random uncertainty from (2)

$$U_r = 3{,}25 \cdot \frac{0{,}13}{\sqrt{1}} = 0{,}42\% \tag{15}$$

The comparison uncertainty is then

$$U_c = \sqrt{U_r^2 + U_s^2} = 0{,}82\% \tag{16}$$

The total uncertainty can now be found by including the uncertainty given for the reference transducer (e_7):

$$U_t = \sqrt{U_c^2 + e_7^2} = 1{,}02\% \tag{17}$$

at the Confidence Level of 99%.

Back-to-Back Comparison Calibration by Using FFT Analysis Method

Modern analysis techniques have made it possible to expand accurate back-to-back calibration over a wide frequency range without a large increase in calibration time. Simultaneously, the demands for more elaborate documentation on measurements and calibrations have increased over the last few years.

To fulfil these requirements a system like the one shown in Fig. 4 has been demonstrated to be useful. The Brüel & Kjær Dual Channel Signal

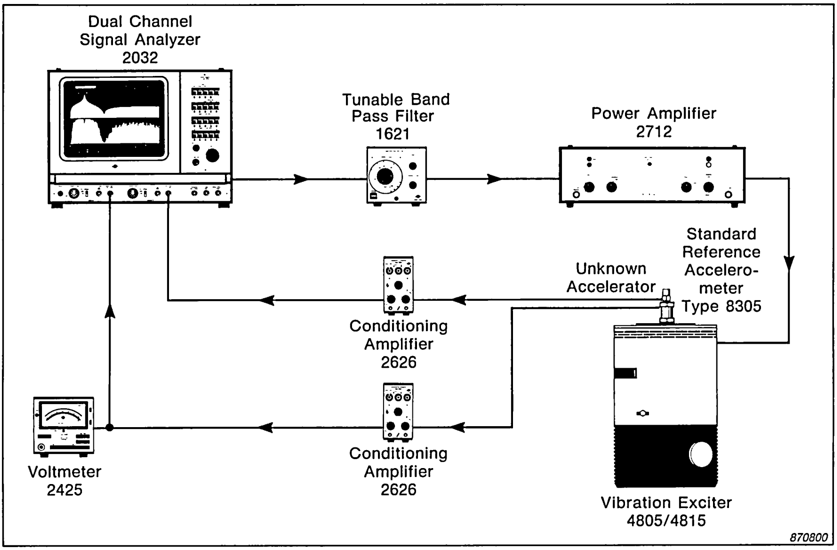

Fig. 4. Back-to-back FFT calibration using random excitation

Analyzers Type 2032/34 perform the comparison at 800 frequencies and provide an excitation signal of random nature covering all these frequencies.

Fig. 5 shows the principle and the formula for the ratio of the sensitivities which now is a function of the frequency f:

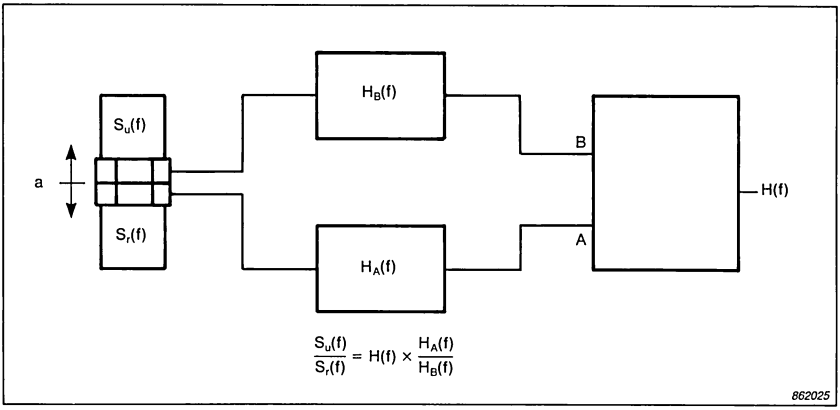

Fig. 5. Working principle of simple FFT calibration

$S_u(f)$ is the charge sensitivity of the unknown accelerometer

$S_r(f)$ is the charge sensitivity of the reference accelerometer

$H(f)$ is the frequency response function value (analyzer readout)

$H_A(f)$ is the frequency response function of the signal-conditioning amplifier in Channel A

$H_B(f)$ is the frequency response function of the signal-conditioning amplifier in Channel B

If the set-up is used in the simplest direct way, provided that the dynamic range of the analyzer is used properly, we can give the resulting uncertainty of a calibration of one Standard Reference accelerometer against another at 160 Hz by using the uncertainties given in Table 3.

e_1	Dual Channel Signal Analyzer Type 2032 Max. error	± 3,1%
e_2	Type 2626 Charge Amplifier (Ch.A) Max. error	± 0,5%
e_3	Type 2626 Charge Amplifier (Ch.B) Max. error	± 0,5%
e_4	Type 8305 Standard Reference Accelerometer sensitivity error due to temperature variation in the range 23°C ± 3°C	± 0,1%
e_5	Type 8305 Standard Reference Accelerometer Error due to transverse vibration (max. 10%)	± 0,2%
e_6	Unknown Accelerometer Output Error due to transverse vibration (max. 10%) Transverse sensitivity max. 2%	± 0,2%
e_7	Unknown Accelerometer Output Error due to difference between room temperature measured and temperature of unknown accelerometer (± 3°C)	± 0,1%
e_8	Calibration uncertainty of 8305 (99% CL)	± 0,6%
σ	Estimated standard deviation calculated from ten consecutive measurements	± 0,1%

T01371GB1

Table 3. Uncertainties, simple FFT calibration (two Standard Reference Transducers Type 8305 at 160 Hz)

From (3) we obtain the systematic uncertainty:

$$U_s = \frac{K}{\sqrt{3}} \sqrt{e_1^2 + e_2^2 + e_3^2 + e_4^2 + e_5^2 + e_6^2 + e_7^2} = 4{,}8\% \text{ at } 99\% \text{ CL} \quad (18)$$

The random component of uncertainty for one measurement ($n = 1$) is:

$$U_r = 0{,}33\% \text{ at } 99\% \text{ CL} \quad (19)$$

The uncertainty of the comparison calibration measurement for $n = 1$ is:

$$U_c = \sqrt{U_r^2 + U_s^2} = 4{,}81\% \text{ at } 99\% \text{ CL} \quad (20)$$

The total uncertainty of the calibration is:

$$U_t = \sqrt{U_c^2 + e_8^2} = 4{,}85\% \text{ at } 99\% \text{ CL} \quad (21)$$

Although 5% is sufficient for many purposes it is often desirable to improve the accuracy. To do so two self-correcting methods will be shown.

Improved FFT Calibration by Switching

Once one measurement has been made as described above, making a second measurement with identical set-up but interchanged cable connections at the transducers will permit cancellation of most of the systematic uncertainties.

Denoting the two frequency response functions $H_{u/r}(f)$ and $H_{r/u}(f)$ we have

$$\frac{S_u(f)}{S_r(f)} = H_{u/r}(f) \cdot \frac{H_A(f)}{H_B(f)} \tag{22}$$

and

$$\frac{S_r(f)}{S_u(f)} = H_{r/u}(f) \cdot \frac{H_A(f)}{H_B(f)} \tag{23}$$

giving

$$\frac{S_u(f)}{S_r(f)} = \sqrt{\frac{H_{u/r}(f)}{H_{r/u}(f)}} \text{ or } S_u(f) = S_r(f) \cdot \sqrt{\frac{H_{u/r}(f)}{H_{r/u}(f)}} \tag{24}$$

The uncertainties are in this case:

e_1	Dual Channel Signal Analyzer Type 2032 (Amplitude resolution) Max. error	± 0,1%
e_2	Standard Accelerometer Type 8305 Sensitivity error due to temperature variation in the range 23°C ± 3°C	± 0,1%
e_3	Standard Accelerometer Type 8305 Error due to transverse vibration (max. 10%)	± 0,2%
e_4	Unknown Accelerometer Output Error due to transverse vibration (max. 10%)	± 0,2%
e_5	Unknown Accelerometer Output Error due to difference between measured room temperature and temperature of the unknown accelerometer (± 3°C)	± 0,1%
σ	Estimated standard deviation obtained by ten consecutive measurements	± 0,1%

T01372GB1

Table 4. Uncertanties, FFT calibration by switching (two Standard Reference Transducers Type 8305 at 160 Hz)

and assuming that transverse movements and temperature do not change between the two measurements, we can find the systematic uncertainty:

$$U_s = \frac{K}{\sqrt{3}} \sqrt{\left(\frac{1}{2} \cdot e_1\right)^2 + \left(\frac{1}{2} \cdot e_1\right)^2 + e_2^2 + e_3^2 + e_4^2 + e_5^2} \tag{25}$$

$$U_s = \frac{2{,}58}{\sqrt{3}} \cdot 0{,}324\% = 0{,}48\% \tag{26}$$

where the two ½ e_1 comes from each H in the formula and ½ from the fact that they are under the square root sign according to the law of propagation of variance, i.e. by using the expansion :

$$Y(x_1, x_2 \ldots x_n) \approx Y(\bar{x}_1, \bar{x}_2 \ldots \bar{x}_n)$$
$$+ \left[\frac{\delta Y}{\delta x_1} \Delta x_1 + \frac{\delta Y}{\delta x_2} \Delta x_2 + \ldots\ldots \frac{\delta Y}{\delta x_n} \cdot \Delta x_n \right] \tag{27}$$

around the mean values $\bar{x}_i$ leading to the expression

$$\sigma_Y^2 = \sum_{i=1}^{n} \left(\frac{\delta Y}{\delta x_i}\right)^2 \cdot \sigma_i^2 \tag{28}$$

where σ_i^2 is the variance of the variable x_i [8].

Similarly, we obtain for the random uncertainty

$$U_r = \frac{3{,}25}{\sqrt{1}} \sqrt{\left(\frac{1}{2}\sigma\right)^2 + \left(\frac{1}{2}\sigma\right)^2} = 0{,}23\% \text{ at } 99\% \text{ CL} \tag{29}$$

From this the comparison uncertainty becomes:

$$U_c = \sqrt{0{,}48^2 + 0{,}23^2} = 0{,}53\% \tag{30}$$

and the total uncertainty

$$U_t = \sqrt{0{,}53^2 + 0{,}6^2} = 0{,}8\% \text{ at } 99\% \text{ CL} \tag{31}$$

Improved FFT Calibration by Substitution

This method is also based on two measurements but in this case one transducer remains fixed to the exciter while a reference and an unknown transducer are compared to it, as shown in Fig. 6.

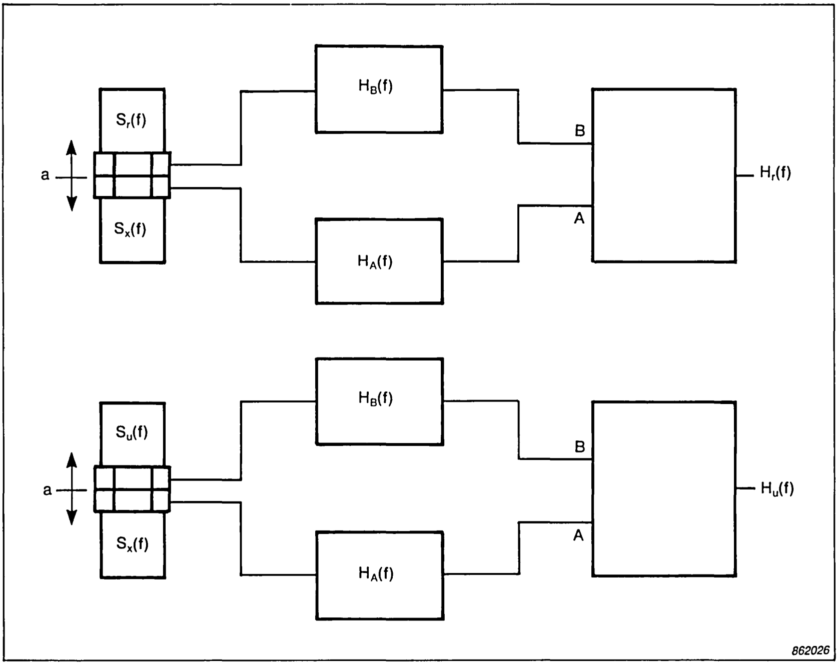

Fig. 6. Working principle of FFT calibration by substitution

It is immediately seen that

$$\frac{S_u(f)}{S_x(f)} \cdot \frac{S_x(f)}{S_r(f)} = \frac{S_u(f)}{S_r(f)} = \frac{H_u(f)}{H_r(f)} \text{ or } S_u(f) = S_r(f) \cdot \frac{H_u(f)}{H_r(f)} \qquad (32)$$

Where:

$S_u(f)$ = Charge sensitivity of the unknown accelerometer
$S_r(f)$ = Charge sensitivity of the primary standard accelerometer

$S_x(f)$ = Charge sensitivity of the reference accelerometer for the measurement
$H_u(f)$ = Frequency response function for the unknown accelerometer relative to the reference accelerometer
$H_r(f)$ = Frequency response function for the primary standard accelerometer relative to the reference accelerometer

The uncertainties are

e_1	Dual Channel Signal Analyzer Type 2032 (Amplitude resolution) Max. error	± 0,1%
e_2	Standard Accelerometer Type 8305 Sensitivity error due to temperature variation in the range 23°C ± 3°C	± 0,1%
e_3	Standard Accelerometer Type 8305 Error due to transverse vibration (max. 10%)	± 0,2%
e_4	Unknown Accelerometer Output Error due to transverse vibration (max. 10%)	± 0,2%
e_5	Unknown Accelerometer Output Error due to difference between measured room temperature and temperature of the unknown accelerometer (± 3°C)	± 0,1%
e_6	Error due to transverse sensitivity of reference transducer and change in transverse vibration (max. 5%)	± 0,1%
σ	Estimated standard deviation obtained by ten consecutive measurements of H	± 0,1%

T01373GB1

Table 5. Uncertainties, FFT calibration by substitution (two Standard Reference Transducers Type 8305 at 160 Hz)

Following the same rules as above, we obtain

$$U_s = \frac{K}{\sqrt{3}} \sqrt{e_1^2 + e_1^2 + e_2^2 + e_3^2 + e_4^2 + e_5^2 + e_6^2}$$

$$= \frac{2{,}58}{\sqrt{3}} \cdot 0{,}36 = 0{,}54\% \text{ at } 99\% \text{ CL} \qquad (33)$$

$$U_r = \frac{3,25}{\sqrt{1}} \cdot \sqrt{\sigma^2 + \sigma^2} = 0,46\% \text{ at } 99\% \text{ CL} \tag{34}$$

$$U_c = \sqrt{0,54^2 + 0,46^2} = 0,71\% \text{ at } 99\% \text{ CL} \tag{35}$$

$$U_t = \sqrt{0,71^2 + 0,6^2} = 0,93\% \text{ at } 99\% \text{ CL} \tag{36}$$

Conclusions

It is demonstrated that self-correcting methods, in conjunction with modern signal analyzers, can improve the accuracy of comparison measurements so that they are better or comparable to dedicated comparison systems. If calibration of Standard Reference Accelerometers is performed in a wider frequency range, and if well-designed systems, including exciters and fixtures, are used, accurate and very fast calibration can be made in the range 5 Hz to 5 kHz by means of the substitution method. If computers are used to generate the set-ups etc., a very powerful documentation system can be made.

To verify the validity of the switching and the comparison by substitution methods, a comparison of the two methods against the Laser Interferometer Method was conducted at six different frequencies from 100 Hz to 650 Hz. Two standard Reference Transducers Type 8305 were used.

It was found that the maximum deviation between the three measurements was in the order of 0,1%. The comparison measurements were conducted in a well-controlled laboratory environment and great care was taken to avoid spurious effects.

Over a period of eight months a large number of accelerometer calibrations were performed by using the comparison-by-substitution method. The measurements were performed under a wide variety of environmental conditions and after transport of the equipment either by road or by air [9].The results were consistent with the uncertainties given in this paper.

References

[1]	NMAS	National Measurement Accreditation Service, *"The Expression of uncertainty in Electrical Measurements"*, B 3003 Fourth Issue, April 1986
[2]	Hohmann, P.	*"Schwingungsmessungen mit Laserinterferometern zur Kalibrierung von Aufnehmern"*, Acustica, Vol. 26 (1972), pp.122–136
[3]	Hohmann, P. & Martin, R.	*"Kalibrierung eines Schwingungsaufnehmer-Vergleichsnormal"*. Physikalisch-Technische Bundesanstalt, Braunschweig (1968), VDI–Berichte Nr. 135 (1969)
[4]	Deferrari, H.A., Darby, R.A. & Andrews, F.A.	*"Vibrational Displacement and Mode-Shape Measurement by a Laser Interferometer"*, Journal of the Acoustical Society of America, Vol. 52, 5, p.982 (1967)
[5]	Actley, R.A. & Logue, S.H.	*"A Laser Interferometer and its applications to vibration amplitude measurement"*, Institute of Environmental Sciences (1967), Proceedings, pp. 235–240
[6]	Licht, T.	Brüel & Kjær, Technical Review No. 1, p.71
[7]	ISO	International Standard Organization, ISO 5347, *"Methods of calibration of vibration and shock pick-ups"*, to be published 1987
[8]	Hanneman, H.W.	*"The Systematic and Random Errors due to Element Tolerances of Electrical Networks"* Philips Research Reports, Eindhoven, pp.414–423, 1971
[9]	Schoenthall,E.	Private Communication

Previously issued numbers of Brüel & Kjær Technical Review

(Continued from cover page 2)

4-1981 Low Frequency Calibration of Acoustical Measurement Systems.
Calibration and Standards. Vibration and Shock Measurements.
3-1981 Cepstrum Analysis.
2-1981 Acoustic Emission Source Location in Theory and in Practice.
1-1981 The Fundamentals of Industrial Balancing Machines and Their Applications.
4-1980 Selection and Use of Microphones for Engine and Aircraft Noise Measurements.
3-1980 Power Based Measurements of Sound Insulation.
Acoustical Measurement of Auditory Tube Opening.
2-1980 Zoom-FFT.
1-1980 Luminance Contrast Measurement.
4-1979 Prepolarized Condenser Microphones for Measurement Purposes.
Impulse Analysis using a Real-Time Digital Filter Analyzer.
3-1979 The Rationale of Dynamic Balancing by Vibration Measurements.
Interfacing Level Recorder Type 2306 to a Digital Computer.
2-1979 Acoustic Emission.
1-1979 The Discrete Fourier Transform and FFT Analyzers.
4-1978 Reverberation Process at Low Frequencies.
3-1978 The Enigma of Sound Power Measurements at Low Frequencies.

Special technical literature

Brüel & Kjær publishes a variety of technical literature which can be obtained from your local Brüel & Kjær representative.
The following literature is presently available:

- ○ Mechanical Vibration and Shock Measurements (English), 2nd edition
- ○ Modal Analysis of Large Structures–Multiple Exciter Systems (English)
- ○ Acoustic Noise Measurements (English), 3rd edition
- ○ Architectural Acoustics (English)
- ○ Noise Control (English, French)
- ○ Frequency Analysis (English)
- ○ Electroacoustic Measurements (English, German, French, Spanish)
- ○ Catalogues (several languages)
- ○ Product Data Sheets (English, German, French, Russian)

Furthermore, back copies of the Technical Review can be supplied as shown in the list above. Older issues may be obtained provided they are still in stock.

Brüel & Kjær

DK-2850 Nærum · Denmark · Telephone: +45 2 80 05 00 · Telex: 37316 bruka dk · Fax.: 02 80 14 05

ISSN 007-2621

BV 0030-11

Printed in Denmark by Nærum Offset